Journal of Oncology Research and Therapy
Singh SS, et al. J Oncol Res Ther 6: 10120.
www.doi.org/10.29011/2574-710X.10120
www.gavinpublishers.com

OPEN ACCESS

GAVIN PUBLISHERS

Research Article

Cigarette Smoke Extract induces Alpha-Enolase by inhibiting Prolyl-Hydroxylases in Cervical Cancer Cells. A comparative study of Reference cigarettes and E-cigarettes

Surya S. Singh[1], Divya J. Reddy[1], Ravikumar Eslavath[2], Wasia Rizwani[1*]

[1]Department of Biochemistry, Osmania University, Hyderabad, Telangana, India

[2]Alphores Junior College, Karimnagar, Telangana, India

[*]**Corresponding author**: Wasia Rizwani, Department of Biochemistry, Osmania University, Hyderabad, Telangana, India.

Citation: Singh SS, Reddy DJ, Eslavath R, Rizwani W (2021) Cigarette Smoke Extract induces Alpha-Enolase by inhibiting Prolyl-Hydroxylases in Cervical Cancer Cells. A comparative study of Reference cigarettes and E-cigarettes. J Oncol Res Ther 6: 10120. DOI: 10.29011/2574-710X.10120

Received Date: 15 December, 2021; **Accepted Date:** 21 December, 2021; **Published Date:** 24 December, 2021

Abstract

Cigarette Smoke (CS) is a major contributor to the development of a large number of fatal and debilitating disorders. Proteomic analysis was used as an investigative tool to systematically explore proteomic changes that contribute to alterations in the cellular milieu leading to progression of cancer upon CS exposure. In this study, we utilized Two-Dimensional Gel Electrophoresis (2-DE) and Mass Spectrometry (MS) technologies to explore protein changes in cervical cancer cells (HeLa) in response to cigarette smoke extract (CSE) exposure. Among the individual proteins resolved using 2DE, about 50 protein spots were analysed by MALDI-TOF/TOF in the first attempt. Proteins related to tumor microenvironment, chronic obstructive pulmonary disease and metastasis induction among others were identified. Of these, alpha-enolase, a multi-functional, yet predominantly a glycolytic enzyme that facilitates aerobic glycolysis through a process known as Warburg effect in cancers, was a prominent protein detected with significant change. Although this protein is known to be induced in cancers, it was not known to be altered by cigarette smoke exposure in cervical cancers. Mechanism-wise CSE induced and stabilized HIF-1a by inhibiting HIF-PH (prolyl-hydroxylases) and thereby, inducing alpha-enolase production in cervical cancer cells. The precise molecular mechanisms underlying the effects of CS in cervical disease are largely unknown. Further investigation on CSE treatment under non-hypoxia conditions *in vitro* and *in vivo* along with proteomic approach may potentially lead to new therapeutic approaches to smoking induced advancement of cervical cancer. The evidence warrants further investigation to indicate that Enolases play an important role in CS-induced gene expression and could be a potential therapeutic target to prevent cancer progression and metastasis.

Keywords: Cigarette smoke; E-cigarettes; Nicotine; Enolase; HRE; HIF-PH; MALDI-TOF/TOF

Abbreviations

HIF-PH: Hypoxia-inducible factor-Prolyl Hydroxylases; **HRE:** Hypoxia Response Element

MALDI-TOF/TOF: Matrix Assisted Laser Desorption Ionization-Time of Flight/Time of Flight

Introduction

Cervical cancer stands out to be the second most frequent cancer in women world-wide. Annual incidences reach about 9 million women of which 80% women are from developing countries [1]. Cervical Intraepithelial Neoplasia (CIN) constitutes a premalignant lesion that precedes the development of cervical cancer. Women who smoked tobacco developed high-grade intraepithelial neoplasia of the cervix. Synergy was observed between severe smoking and the use of oral contraceptives, with

a greater risk of grade II and III intraepithelial neoplasia [1]. Cervical cancer is the leading cause of cancer deaths in both rural and urban areas in India. Tobacco smoke is a complex mixture of over 5,000 identified chemicals, of which 98 are known to have specific toxicological and carcinogenic properties [2-5]. Tobacco use leads to a major risk factor for heart attacks, strokes, Idiopathic Pulmonary Fibrosis (IPF), Chronic Obstructive Pulmonary Disease (COPD), Emphysema and cancer. The most important chemicals causing cancer are those that produce DNA damage since such damage appears to be the primary underlying cause of cancer [6]. The smoke from tobacco elicits carcinogenic effects resulting in combustion, pyrolysis and other chemical reactions. The damaging effects of tobacco smoking are dose-dependent as both active and passive smoking can cause disease not only in organs directly exposed to tobacco smoke, such as the mouth and lung, but also in distant organs such as the bladder, colon, breast and also cervical cancer. These harmful substances are absorbed through the lungs and carried in the bloodstream throughout the body [6]. Smokers are about twice as likely as non-smokers to get cervical cancer. Tobacco by-products have been found in the cervical mucus of women who smoke. Researchers believe that these substances damage the DNA of cervix cells and may contribute to the development of cervical cancer. Smoking also makes the immune system less effective in fighting HPV infections.

Smoking related cervical carcinogenesis may be due to multiple mechanisms: one involving direct exposure of the Deoxyribonucleic Acid (DNA) in cervical epithelial cells to nicotine and cotinine, and the other involving exposure to metabolic products resulting from the reactions of other components of cigarettes such as aromatic polycyclic hydrocarbons and aromatic amines [7,8]. It has been observed that cervical mucus of smokers contain measurable amounts of cigarette constituents and their metabolites such as benzo[a]pyrene (BaP) [9], nicotine, and nicotine derived nitrosamines 4-(methylnitrosamino)-1-(3-pyridyl)-1-butanone [10]. BaP up-regulation of HPV genome amplification may increase the probability of viral DNA integration into the host genome, a milestone in the development of cervical cancer [11]. It has been suggested that in vivo effects of long-term nicotine exposure could affect persistent cellular proliferation, inhibition of apoptosis, and stimulation of vascular endothelial growth factor, with increased microvessel density [12].

In an attempt to identify novel biomarkers in cervical cancer cells exposed to CSE through proteomic analysis, we identified Enolase to be an important biological molecule that could possibly be facilitating sustenance of cancerous state. Enolase has been found to be a promising therapeutic as well as diagnostic tumor target. Hence, we further investigated partially the mechanism it adopts to help cancer cells survive in CSE-induced stress.

Enolase was initially typified as an enzyme involved in glucose metabolism. Its three isoforms, namely, α- (ENO1), β- (ENO3), and γ- (ENO2) enolase forms homodimers or heterodimers to convert 2-phosphoglycerate into phosphoenolpyruvate in the glycolytic pathway. Multiple evidences, however, indicate that α-enolase is a multifunctional protein [13]. In addition to its glycolytic function, which is primarily exerted in the cytoplasm, α-enolase has been found on the cell surface, where it functions as a plasminogen receptor, implying that membrane-bound enolase may play a role in inflammation and tissue invasion [14]. In hypoxic situations, α-enolase also acts as a stress protein and it has been speculated that its up-regulation may provide protection to cells by increasing anaerobic metabolism [15]. Changes in ENO1 gene expression have been observed in several cancer cell models, whereas the clinical correlation of ENO1 expression to tumor status has not yet been clearly defined. Up-regulation of ENO1 has been reported in several highly tumorigenic or metastatic cell lines derived from alveolar type II pneumocytes [16], small cell lung cancer [17], head and neck cancers [18]. Similarly, studies examining enzymatic activities in breast cancer indicated a role for α-enolase in tumor progression [19]. Two recent studies, one reporting the overexpression of α-enolase in 18 out of 24 different types of cancer including breast cancer [20] and the other demonstrating the association of phosphorylated isoforms with pancreatic ductal adenocarcinoma [21], further support a correlation between ENO1 expression and its general pathophysiological role in cancer formation. HIF-1 is one of the most important transcription factors responsible for hypoxia-induced gene expression. In our present study, we found both ENO1 and HIF-1a exhibit enhanced expression in response to reference-research cigarettes and E-cigarettes suggesting that nicotine might exert these effects in cervical cancer cells. Response to radiation is diminished in cervical cancer patients with high HIF-1a expression [22]. We believe that a combined inhibition of Enolases and HIF-1a could prevent cancer progression significantly.

Materials and Methods

Cell Culture

Immortalized human cervical cancer cell lines (Hela) were purchased from National Centre for Cell Science (NCCS), Pune. HeLa cells were maintained in RPMI-1640 (PAN Biotech) containing 10% fetal calf serum (Gibco) and 1% antibiotic-antimycotic solution (HiMedia). Cells were cultured at 37 °C in a humidified 5% CO_2 incubator.

Preparation of Cigarette Smoke Extract (CSE)

Research-reference cigarettes (2R4F, 0.8 mg Nicotine/cig/10 puffs) were obtained from Kentucky Tobacco Research and Development Centre at the University of Kentucky. Disposable E-cigarettes (Brand Tsunami) were from a store in New Jersey, USA. CSE from Research-Reference Cigarettes (RRC) and

E-cigarette (EC) was prepared according to Luppi, et al. method [23]. CSE (100%) stock was prepared by bubbling one cigarette smoke through 10 ml of PBS via 50ml sterile syringe. This CSE stock was then filtered using a 0.22µm filter from BD Biosciences filter to remove particles and bacteria. CSE concentration was diluted according to the requirement (of experiment) with media. The 100% CSE prepared by this procedure described above is estimated to represent approximately 1/3 of a smoker's plasma concentration of soluble cigarette smoke contents. E-Cigarette smoke extract was prepared to match the nicotine concentration in RRC.

Cell Viability Assay

To determine cell viability [24] at various concentrations of CSE (0, 1, 2, 3, 4, 5, 6,7,8,9, 10%) exposure, 10,000 cells were plated in triplicate in 96-well plates and cell viability was assessed by MTT (3-[4,5-dimethylthiazol-2-yl]- 2,5-diphenyltetrazolium bromide) assay at 24hr of CSE treatment. MTT reagent (diluted from a 4 mg/ml solution in PBS) was added to all the wells at a final concentration of 0.4 mg/ml and the cells were further incubated for 4hr at 37 ^{0}C. The reaction was terminated by adding 200 µl/well dimethyl sulfoxide (DMSO, Sigma) and absorbance was read at 570 nm in an ELISA plate reader (Thermo Scientific Multiskan EX). Wells containing serum-free media alone was used as blank and the average values subtracted from the average values of all clones. The assay was repeated three times and analysed using two-sided Student's t test. Data points represent the mean ± s.d and $p<0.05$ was considered significant.

2-Dimensional Polyacrylamide Gel Electrophoresis (2D-PAGE)

Sample Preparation

For 2D-PAGE analysis, HeLa cells were grown to 80% confluency and treated with 5% CSE from RRC for 16h or left untreated (Control sample) for normoxia cells were incubated to 5% CO_2 maintaining 37 ˚C. Cells were trypsinized, collected and washed twice by centrifugation in phosphate buffered saline (PBS, pH 7.2). Approximately 2×10^6 cells were lysed in 1ml lysis buffer (7M urea, 20 mM Thiourea, 4% CHAPS, 10 mM DTT, 1 mM EDTA, 1 mM PMSF 0.2% pH 3–10 ampholytes; BioRad, USA) containing protease inhibitor cocktail 8340 (Amresco). Samples were then kept on ice and sonicated in six cycles of 10s, each consisting of 5s sonication followed by a 10s break. After centrifugation at 14,000 rpm for 1h at 4 ˚C, the supernatant was collected and the protein concentrations were determined using the Bradford protein assay (Manufacturer's protocol).

Two- Dimensional Electrophoresis

Protein samples (3 mg) were applied to an immobilized pH gradient (IPG) strip (17cm, pH 3–10 NL, BioRad, USA) using a passive rehydration method. After 12–16 h of rehydration, the strips were transferred to an Isoelectric Focusing (IEF) cell (BioRad) and focused for a total of 60 000 V-Hr. The second dimension was performed using 9-16% gradient SDS-PAGE at 24 mA/gel after equilibration. The following proteins were added as molecular weight markers: myosin (220000), phosphorylase A (94 000), catalase (60 000), actin (43 000), carbonic anhydrase (29 000) and lysozyme (14 000). The gels were stained using CBB R-250 (Merck, Germany) for 48 hr, gels were fixed in solution composed of 50%(v/v) methanol and 12%(v/v) acetic acid for 1hr. The gels were de-stained in MQ water.

Gel Imaging and Analysis

The two-dimensional gels were scanned and images obtained using GE Image Scanner III Lab Scan 6.0. To study and compare the differences in the protein expression profile of CSE-treated and untreated (control) HeLa samples, gels were analysed with Image Master 2D platinum Software 7.0 (GE Healthcare).

The general method of computerized analysis for the paired experimental and control gels included automatic spot finding and quantification, automatic background subtraction (mode of non-spot) and automatic spot matching in conjunction with detailed manual checking of the spot finding and matching functions. The spot % volumes were normalized using the ratio method of normalization in the software. The fold changes were calculated using average means of normalized % spot volume of duplicate 2-D gels. The p-values for treated and control were calculated by Graph pad software (version 5.0) using student's t-test. The molecular weight and pI values for each spot were determined from algorithms applied to the reference image.

In-Gel Digestion

In-gel digestion of proteins was carried out using MS-grade Trypsin (SIGMA) according to the manufacturer's instructions. Briefly, spots of interest were cut out of the gel (1–2 mm diameter) using a razor blade, and destained twice with 100 mM NH_4HCO_3/50% acetonitrile (ACN) at 37 ^{0}C for 45min in each treatment. After dehydration and drying, the gels were pre-incubated in 10–20 µl trypsin solution for 30min at 37 ^{0}C. Then samples were added in adequate digestion buffer (25 mM NH_4HCO_3/10% ACN) to cover the gels and incubated overnight at 37 ˚C. Tryptic digests were extracted using 3:1 acetonitrile/TFA (trifluoroacetic acid), followed by sonication for 30 min at 37 ^{0}C extraction twice with 25ul of 50% (v/v) ACN/5%(v/v) TFA to each gel for 1hr each time. The combined extracts were dried in a vacuum concentrator at room temperature. The samples were then subjected to MS analysis.

MALDI-Q-TOF Analysis And Protein Identification

Mass spectra were acquired using a MALDI time-of-flight / time-of-flight (MALDI-TOF/TOF) mass spectrometer

(Bruker,UK) with a matrix-assisted laser desorption ionization (MALDI) source (Micromass). Tryptic digests were dissolved in 5 µl of 70% ACN/0.1% TFA, and then 1 µl of the digests was mixed with 1 µl saturated alpha-cyano-4-hydroxy-cinnamic acid (CHCA) in 50% ACN/0.5% TFA and spotted onto a 96- well target plate and allowed to dry.

Before analysis the instrument was calibrated with mass standards: Bradykinin (m/z 757.39), Angiotensin II (m/z 1046.54), Angiotensin I (m/z 1296.68), substance p (m/z1347.33), Bombysin (m/z 1619.82), ACTH fragment 1-17(m/z 2093.08), fragment 18-39 (m/z 2465.39), Somatostatin (m/z 3147.47). Spectras were obtained in the reflectron mode (mass range from 500-3000Da, 20KeV accelerating voltage, and averaging 500 laser shots per spectrum) using MALDI-TOF/TOF spectrometer with Flex Control Software (Version 3.3 Bruker Daltonics). For PMF, the generated peptide mass list were exported to Biotools software (version 3.3, Bruker Daltonics) with the following parameters: signal-to-noise (S/N) threshold, 6; Mass Exclusion Tolerance, 0.75m/z; Maximal number of peaks, 100; Quality Factor Threshold, 50; Monoisotopic peaks (Adduct:H). Matrix and auto-proteolytic trypsin peaks or known contaminant ions were excluded.

Bioinformatics data mining was performed using in-house licensed version of the MASCOT database search engine (Matrix science, Boston, MA). The SWISS-PORT Database searches were carried out using the following parameters: database, Swiss-Prot; taxonomy, Homo sapien; enzyme, trypsin; and allowance of one missed cleavage. Protein that returned MOWSE scores over a threshold of 50 were considered significant. Further analysis and function based classification of identified proteins was performed using the Protein Centre software version 3.10 by Thermo Fisher Scientific.

Luciferase reporter assay

HeLa cells (1 X 10^4) were co-transfected with 2µg of HRE Luciferase reporter vector (p GL 4.42[Luc 2p/ HRE/ Hygro] vector) and RLuc vectors according to the manufacturer's protocol followed by treatment with different concentrations of RRC- and EC-CSE and no inhibitor or PHD inhibitor (0.5mM DMOG) for 24 hrs. After treatments, cells were washed with cold PBS (pH 7.2) and lysed with 200 ml of lysis buffer (25 mM Tris pH-7.8, 2 mM DTT, 2 mM EDTA, 10% glycerol, 1% Triton X-100) for each well and centrifuged at 2000rpm for 10min at 4 ^{0}C. Supernatant collected was mixed with Luciferase assay reagent (25 mM Tris pH-7.8, 20mM $MgSO_4$, 4mM EDTA, 1 mM DTT, 0.5 mM D-Luciferrin, 2 mM ATP) and luminescence readings were taken with GloMax 20/20 luminometer (Promega, Madison, WI, USA). Luminescence readings were normalized to Renilla Luciferase activity from co-transfected Rluc gene, which is controlled by a constitutive promoter.

RNA purification and Reverse Transcriptase-PCR

HeLa cells were treated with different concentrations of CSE (from RRC and EC) for a period of 16h. Cells were lysed in Tri reagent (Sigma- Aldrich, USA), RNA was extracted in chloroform and precipitated in isopropanol. RNA was suspended in DEPC treated water and quality of RNA was measuring at 260 nm and 280 nm optical densities. RNA (150 ng) was converted into first-strand cDNA using the First Strand cDNA synthesis kit (Fermentas, Burlington, Canada) using Oligo $(dt)_{18}$ primers according to the protocol recommended by the manufacturer. Each PCR reaction was performed in a total volume of 20µl containing 1.0 µl of first-strand cDNA, 1X SYBR Green PCR Master Mix (Applied Biosystem), and 0.5 µM of enolase forward primer (FP: 5' CATGATCCTCCCAGTCGGTG 3') and reverse primer (RP: AGCCAGCTTTCCCAATAGCA). The PCR conditions were 10 minutes at 95 ˚C, 1 minute at 55 ˚C, 40 cycles of 15 seconds at 95 ˚C, followed by 30 seconds at 55 ˚C.

The real-time PCR primers sequences for HIF-1a are Forward Primer-CCAGCAGACTCAAATACAAGAACC and Reverse Primer- TGTATGTGGGTAGGAGATGGAGAT and for Actin are FP: 5' GTGGCCGCTCTAGGCACCA 3' and RP: CGGTTGGCCTTAGGGTTCAGGGGGG 3'. The mRNA expression data were normalized using Actin RNA as internal control, and the fold-change in the expression levels was determined using the quiescent cells as control. GAPDH was also tested as internal control. Each qPCR analysis was performed three independent times.

Statistical Analysis

All tests of statistical significance were two-tailed, p-values less than 0.05 were considered statistically significant.

Results and Discussion

Effect of RR-CSE on cell viability of HeLa cells.

Cell viability of HeLa cells was determined with MTT assay following treatment of cells with various concentrations of Cigarette Smoke Extract (CSE) from Reference-Research (RR) cigarettes for 24 hr. A slight increase in cell growth was observed in cells treated with 1-10% of RR-CSE with maximum effect (upto 27% ± 5% increase) seen at 5% concentration when compared to untreated (control) cells (Figure 1). Hence, 5% RR-CSE was used for analysis of change in expression of proteins by 2D- Gel Electrophoresis. This was done to ensure there is no cell death at the concentrations that will be used in future experiments.

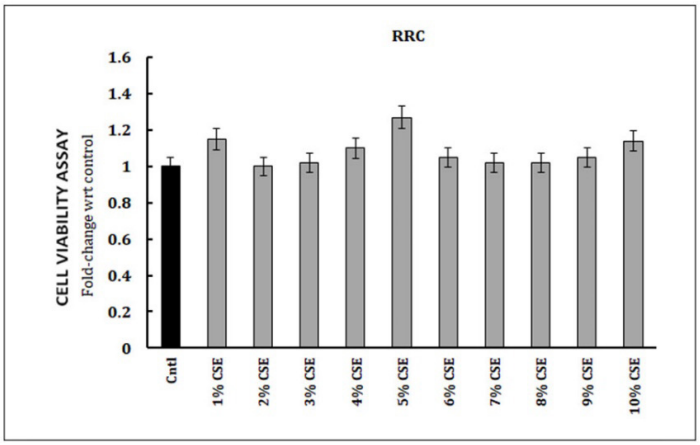

Figure 1.

Figure 1: Enhanced cervical cancer cells viability with exposure to different concentrations of Reference-Research cigarette smoke extract (RR-CSE). MTT assay shows increase in cell growth at 24hr of RR-CSE exposure, maximum effect seen at 5% CSE.

Analysis of changes in protein expression by 2D-GE and MALDI-TOF/TOF, upon exposure to RR-CSE

HeLa cells were exposed to 5% RR-CSE in DMEM media without serum for 16 hr. Untreated cells were used as control. Cell lysates were prepared according to the protocol to run 2D-gel electrophoresis (Figure 2). Following this clear spots were selected and gel pieces were cut to elute out the protein. The protein was digested to obtain peptide fragments that were subjected to MALDI-TOF/TOF for detection and analysis. In the first batch itself, a total of 50 proteins were identified- some were up-regulated in CSE treated cells (Figure 3) and some were down-regulated (Figure 4) while some others remained constant (Table 1). Analysis of 44 proteins (Table 1) with Protein Center Software Version 3.0 from Thermo Scientific was conducted and pie charts were generated based on annotations of gene ontology. Proteins involved in cellular processes like cell death and differentiation; communication, growth and proliferation; transport, stimuli response, defence response and multiplication were highlighted (Supplementary figure 1A). At the molecular level, these proteins were involved in signal transduction, enzymatic activities, DNA and RNA-binding or protein binding functions (Supplementary figure 1B). Protein-protein interactive network data was generated by STRING database and at least 11 proteins showed significant involvement suggesting how many pathways get activated by exposure to CSE within a short time (Supplementary figure 1C). Some of the proteins with enhanced expression were enolases, Heteronuclear Ribonucleoproteins, Heat-shock proteins, MMEL protein, Calreticulin, T-cell receptors, Malate dehydrogenase etc. Vimentin, PRAME family members, Annexin A2 were some of the proteins with decrease in expression upon CSE exposure. It is a well-known fact that Vimentin expression alters with epithelial to mesenchymal cellular transition. Vimentin exhibits reduced expression in epithelial cells as seen in HeLa cells. Continuous exposure to nicotine or CSE can induce mesenchymal phenotype wherein Vimentin expression becomes enhanced leading to tumor progression and metastasis in various cancers and lung tumors [25].

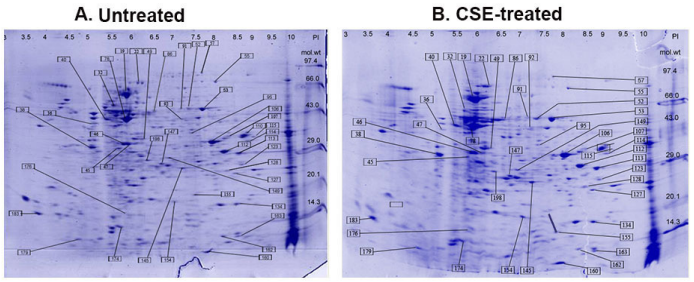

Figure 2

Figure 2: Proteomic spread on 2D-GE upon treatment of HeLa cells with 5% RR-CSE for 16 hr. Untreated cells were used as control in this assay. The gels were stained with Coomassie Blue G250 and de-stained for visible clear spots on 2 dimensional gel. pI strip from 3-10 was used and molecular weight markers were loaded in one of the wells in a vertical run.

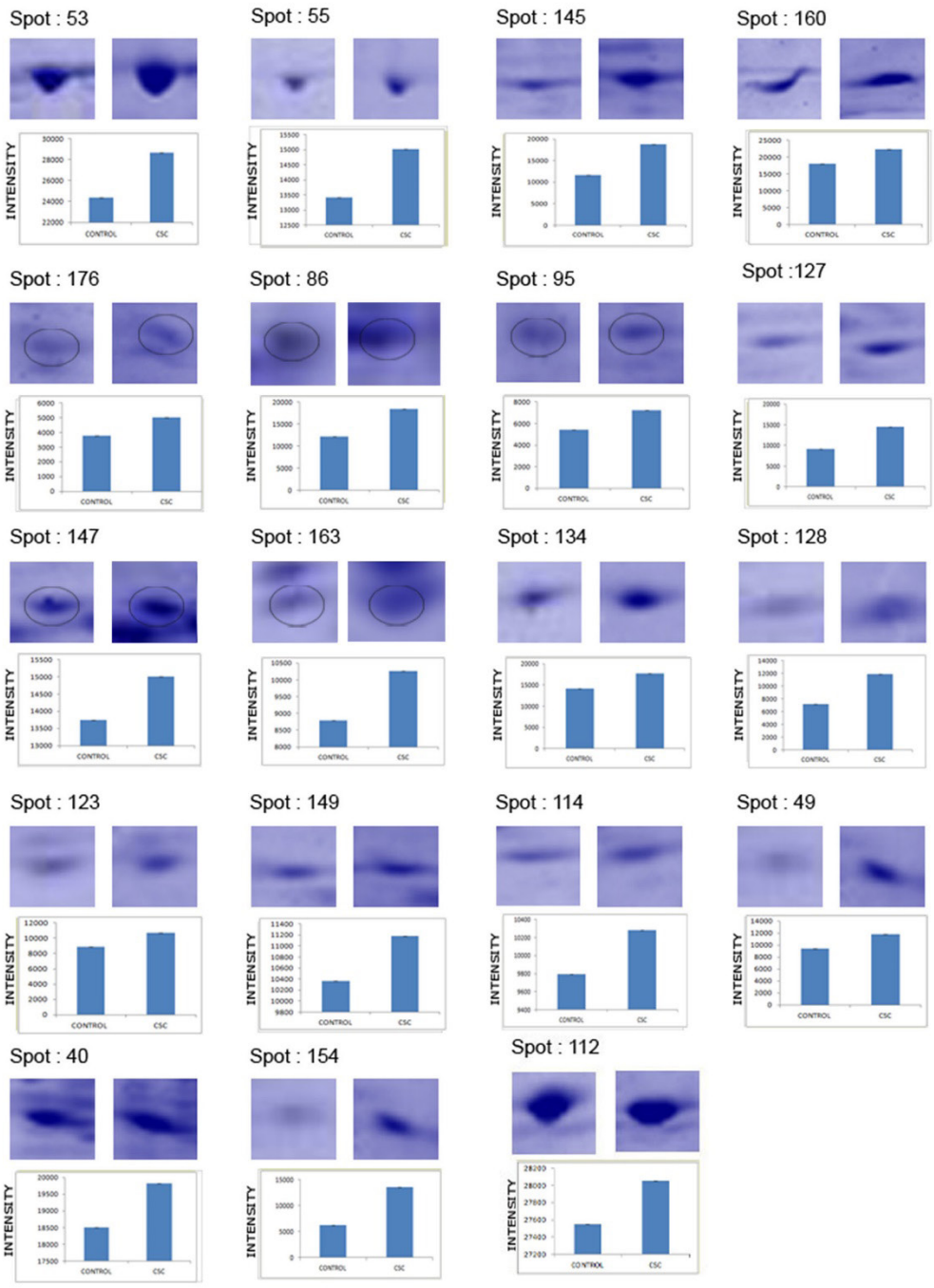

Figure 3.

Figure 3: Identification of some of the up-regulated proteins with MALDI-TOF/TOF and gels were analysed with Image Master 2D platinum Software 7.0 (GE Healthcare) upon treatment with 5% RR-CSE for 16 hr.

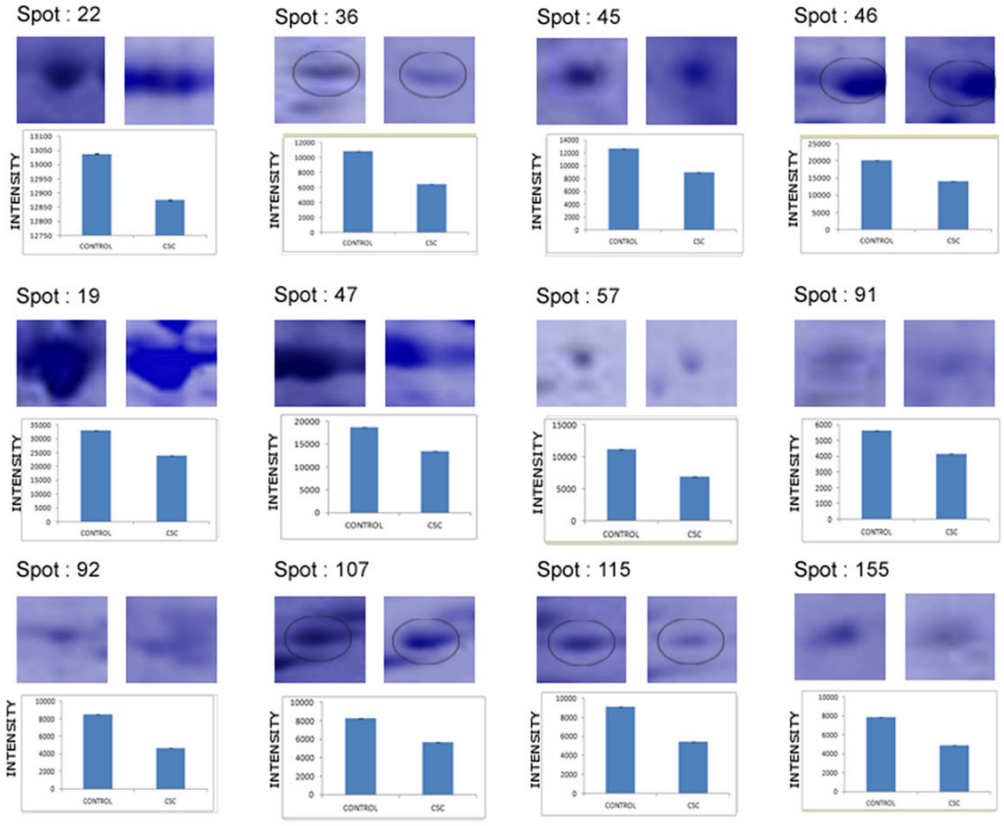

Figure 4.

Figure 4: Identification of some of the down-regulated proteins with MALDI-TOF/TOF and gels were analysed with Image Master 2D platinum Software 7.0 (GE Healthcare) upon treatment with 5% RR-CSE for 16 hr.

S.NO	SPOT NO.	GENE	MW(KDa)	pI	Protein Identified
1	53 (Up)	ENOA_HUMAN	47.4	7.01	Alpha-enolase
2	52 (Up)	ENO1	48	7.4	Chain A, Crystal Structure Of Human Enolase 1
2	100 (Same)	GAPDH	41	8	Glyceraldehyde-3-phosphate dehydrogenase
3	107 (Down)	KCNIP1	35	8.3	Kv channel-interacting protein 1 OS=Homo sapiens
4	145 (Up)	HNRNPH1	24	7.2	heterogeneous nuclear ribonucleoprotein H1 (H), isoform CRA_b

5	176 (Up)	MMEL1	14	**5.8**	MMEL1 protein
6	127 (Up)	PRDX1	21	8.4	peroxiredoxin 1, isoform CRA_b
7	170	ERH	10	6.2	Enhancer of rudimentary homolog
8	164	ATPIF1	11	8.9	ATPase inhibitor, mitochondrial
9	128	SND1-IT1	21	8.3	Susceptibility protein NSG-x
10	163 (Up)	HNRNPH3	14	8.2	heterogeneous nuclear ribonucleoprotein H3 (2H9), isoform CRA_d
11	162	HIVEP1	11	8.2	zinc finger protein 40
12	147 (Up)	HSP27	25	6.7	heat shock protein 27 [Homo sapiens]
13	113	HSPA8	29	9.0	Chain A, Crystal Structure Of Hsc70BAG1 IN COMPLEX WITH ATP
14	86 (Up)	NME2P1	52	6.4	Putative nucleoside diphosphate kinase
15	114 (Up)	MDH2	34	8.9	mitochondrial malate dehydrogenase 2, NAD
16	112 (Up)	GAPDH	29	8.2	glyceraldehyde-3-phosphate dehydrogenase isoform 2
17	160(L7) (Up)	TSG101	14	7.8	Chain B, Tsg101(Uev) Domain In Complex With Ubiquitin
18	160(L7) 2	USP2	10	6.70	Chain B, Crystal Structure Of Usp2 In Complex With Mutated Ubiquitin
19	22 (Down)	HSPA9	81	6.2	stress-70 protein, mitochondrial precursor [Homo sapiens]
20	149 (Up)	TCRB	27	6.9	T cell receptor beta chain [Homo sapiens]
21	92 (Down)	PRAMEF7	43	7.2	PRAME family member 7
22	115 (Down)	ANXA2	35	9.6	Annexin A2
23	40 (Up)		48	5.5	unnamed protein product [Homo sapiens]
24	45 (Down)	HSPA9	30	5.7	Chain A, Substrate Binding Domain Of The Human Heat Shock 70kda
25	49 (Up)	CAPA2A1	36	6.2	F-actin-capping protein subunit alpha-1

26	32	ATP5F1B	50	5.6	mitochondrial ATP synthase, H+ transporting F1 complex beta subunit
27	46 (Down)	SRSF1	34	5.9	splicing factor, arginine/serine-rich 1 (splicing factor 2, alternate splicing factor), isoform CRA_
28	134 (Up)	PP1A 5CYH_A	18	7.8	Chain A, Cyclophilin A Complexed With Dipeptide Gly-Pro
29	160(024)		81.7	5.73	Chain A, Crystal Structure Of Human Ubiquitin In A New Crystal Form
30	198	3TKP	28	6.10	Chain A, Crystal Structure Of Full-Length Human Peroxiredoxin 4 In The Reduced Form
31	183	CAMK2D	16	4.09	Chain D, Crystal Structure Of Su6656-Bound Calcium CALMODULIN- Dependent Protein Kinase II Delta In Complex With Calmodulin
32	74	KRT10	39	4.72	keratin 10, partial [Homo sapiens]
33	121	HMBOX1	34.7	8.81	homeobox containing 1 transcript variant b [Homo sapiens
34	154 (Up)	CALR	30.2	4.74	Chain A, Crystal Structure Of The Globular Domain Of Human Calreticulin
35	123 (Up)	HNRNP A2/B1	31.1		heterogeneous nuclear ribonucleoprotein A2/B1, isoform CRA_d
36	179	UNC13A	19.48	5.21	Protein unc-13 homolog A
37	57 (Down)	PPM1E	85.8	4.96	Protein phosphatase 1E
38	38	TPM4	28.6	4.67	Tropomyosin alpha-4 chain
39	55 (Up)	FUBP1	67.6	7.18	Far upstream element-binding protein 1
40	78 (Same)	ACTB	42	5.29	Actin
41	19 (Down)	HSPD1	61	5.70	60 kDa heat shock protein, mitochondria

Table 1: List of proteins identified from 2D Gel spots by Peptide Mass Fingerprinting with MALDI-TOF/TOF Analysis. Proteins were Up- or down- regulated or remained unchanged in CSE treated gel spots when compared to Untreated control gel spots.

Pathway Analysis: Enolase stood out as the promising protein candidate responding to CSE

Among these, 44 identified proteins were first subjected to enrichment pathway analysis (Supplementary Table 1); 10 independent pathways were detected, of which three were involved in glycolysis. We identified glycolytic protein, Enolase 1 or alpha-enolase as one of the major proteins to be significantly up-regulated. Proteins involved in glycolysis and gluconeogenesis were prominently expressed in CSE-treated cells (Supplementary figure 2). Other prominent pathways activated due to cigarette smoke components are cytoskeletal remodelling pathways, Autophagy and Protein folding. Each pathway can be independently studied to identify novel biomarkers as well as therapeutic targets to prevent initiation or progression of cancers related to cigarette smoking.

Increased expression of Enolase and inhibition of HIF-Prolyl Hydroxylases by CSE

We assessed mRNA levels of alpha-enolase in RR-CSE exposed cells to confirm the 2D-GE results wherein we discovered increase in expression of Enolase 1 at protein level. To establish this, HeLa cells were exposed to RR-CSE at 3%, 5% and 10% CSE for 16 hr and RT-PCR test was conducted using alpha-Enolase primers and Actin primers were used as internal control. The results were compared to untreated cells. There was a significant increase in Enolase mRNA levels at all concentrations tested: a 1.6-fold increase at 3% CSE, 4.4-fold increase at 5% CSE and 8.67-fold at 10% CSE exposure was observed when compared to control cells (Figure 5A). Recent studies show that ENO1 is related to the occurrence and metastasis of malignant tumors. Altenberg and Greulich [26] found increased ENO1 expression on the cell surface of small cell lung cancer cells and head and neck cancer cells through gene chip and Expressed Sequence Tags (ESTs) studies. They showed increased invasive capabilities. Similarly, Fu, et al. [27] established that ENO1 facilitates glycolysis, growth, migration and invasion of small-cell lung cancer cells through a Focal Adhesion Kinase (FAK)-mediated phosphatidylinositol 3-kinase (PI3K)/AKT pathway. On the contrary, patients with non-small cell lung cancer (NSCLC) showing reduced ENO1 expression exhibit a poor prognosis [28]. Interestingly, ENO1 activity was found to be high in migrating breast cancer cells. Also, ENO1 expression is estrogen receptor (ER) dependent, i.e., higher in ER^+ when compared to ER^- breast cancers. Chu, et al. correlated poor prognosis in breast cancer patients with high ENO1 expression levels [29]. As observed from some other studies, enolase expression varies with tumor tissue type or origin. Although Enolases have multiple functions in a cell, its expression can vary in cancers depending on stages of cancer and physiological process of a cell [30]. Increase in cellular glucose presence with a concomitant senescent activity in cisplatin-resistant ovarian cancer cells is associated with reduced expression of enolase-1 [31]. But, overexpression of alpha-enolase is observed in pancreatic and liver cancer [32].

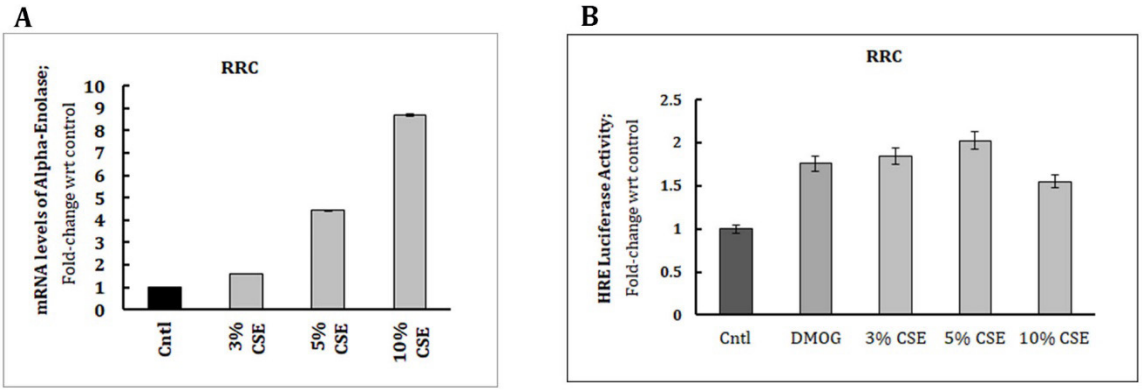

Figure 5.

Figure 5. Alpha-Enolase expression was significantly enhanced upon treatment with various concentrations of RR-CSE (A). RT-PCR analysis was conducted to confirm the data obtained from proteomic analysis. HRE Luciferase Assay revealed CSE acting similar to DMOG, an inhibitor of HIF-PH that prevents degradation of HIF-1a by prolyl-hydroxylase (B).

To further elucidate the mechanism of action of Alpha- Enolase due to cigarette smoke exposure, we performed HRE (Hypoxia Response Element) Luciferase Assay. It is very well established that Hypoxia-inducible factor-1a is induced by both cigarette smoke exposure and its component nicotine. Also both HIF-a and ENO1 are hypoxia-responsive genes. ENO1 promoter consists of HRE consensus sequence 5'-ACGTG-3' to which stabilized HIF-abinds and drives the mRNA synthesis of ENO1. During the local growth of tumor, the surrounding vessels fail to meet the high demand of oxygen leading to hypoxic areas within the tumor and TME [33]. Prolyl-hydroxylases are responsible for the labelling of hypoxia-inducible factors (HIFs) to be degraded by 26S proteasome. Under hypoxic conditions, prolyl-hydroxylases are inhibited, leading to the stabilization of HIFs that induces the expression of various genes implicated in tumor progression. HIF-1a is targeted for destruction in normoxic environments by the hydroxylation of specific proline residue, P564, by the oxygen-sensing enzyme HIF-1a -prolyl hydroxylase (HIF-PH) [34]. DMOG (Dimethyloxallyl glycine) is a cell permeable, competitive inhibitor of HIF-PH. It acts by stabilizing HIF-1a expression at normal oxygen tensions in cultured cells. In this study, we believe that CSE is inducing Enolase by stabilizing HIF-1, which is being facilitated by inhibition of prolyl-hydroxylases.

To prove this, HeLa cells were co-transfected with HRE-Luciferase reporter and Renilla Luciferase vectors followed by CSE treatment for 16 hr. At the same time, co-transfected cells were treated with a known Prolyl-hydroxylase inhibitor DMOG or left untreated (Control). Cells were lysed and luciferase assay was performed. We observed that different concentrations of CSE (3, 5, 10%) acted similar to DMOG in stabilizing HIF-1α, concomitant with increased (2- to 2.5-fold) HRE promoter activity in HeLa cells (Figure 5B). This is a novel finding to deduce the pathway involved in activation of HIF and ENO1 and how tumor cells keep aerobic glycolysis active under normoxic conditions. From the above results, we assume that components of cigarette smoke act to inhibit HIF-PH, stabilize HIF-1α, supports its binding to HRE sequence in ENO1, drives the synthesis of ENO1 mRNA and thereby protein. This in turn facilitates aerobic glycolysis in cells partly. Further studies to elucidate the glycolytic activity and other molecular functions involving Enolase pathway will help us understand how to curb the progression of cancer through Enolase overexpression. HIF-1 is also a key regulator of the metabolic switch. By inducing specific gene expression, it alters the cellular metabolism, increasing glycolysis and lactate production [35]. Lactate arises from glycolysis which takes place under hypoxic conditions, but in tumors glycolysis can also take place in oxygenated areas [35].

Enolase and HIF-1α expression and inhibition of HIF-PH by E-cigarette smoke exposure.

Tumor hypoxia is not static, but evolves and diminishes in a dynamic process depending on tumor growth, neo-angiogenesis, and treatment [36]. Any of the components from RR-cigarette smoke could lead to activation of hypoxia-responsive genes. E-cigarettes are mainly composed of nicotine along with some other non-carcinogenic compounds in liquid form. We conducted same studies using E-cigarettes as we did with RR-cigarettes. It was already established by proteomic study that enolases are up regulated. We first demonstrated that cell viability is good with exposure to different concentrations (1, 2, 3, 4, 5, 6, 7, 8, 9, 10%) of E-CSE (Figure 6A). E-cigarette smoke extract exerted a more pronounced induction of alpha-enolase mRNA levels at 5% (2.6-fold increase) and 10% (10.1-fold increase) CSE exposure of HeLa for 16hr (Figure 6B). Similarly, E-CSE showed a significantly higher HRE promoter activity as compared to DMOG and control (Figure 6C) at the concentrations tested, i.e., 3%, 5% and 10% E-CSE for 16 hr exposure. When HIF-1α message was checked by RT-PCR, HIF-1a induction with E-CSE exposure was evident (Figure 6D). It is safe to conclude that nicotine in E-cigarettes and possibly Reference-cigarettes is the controlling factor to induce hypoxia-responsive genes HIF-1 and ENO1 by inhibiting prolyl-hydroxylases to promote tumorigenesis.

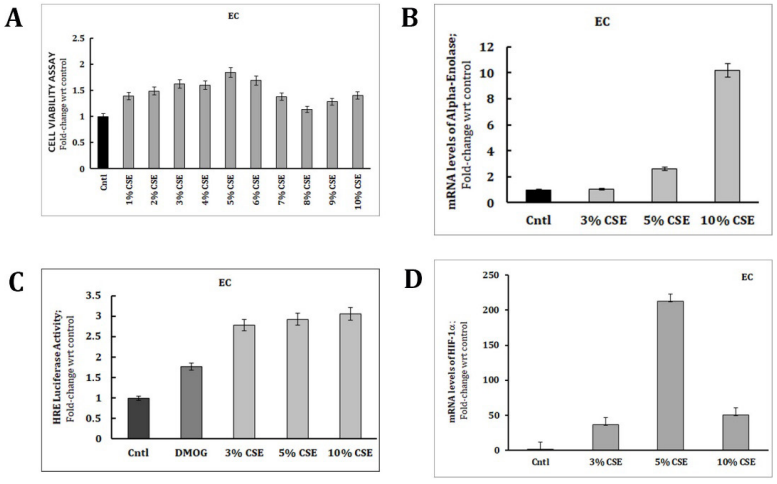

Figure 6.

Figure 6: Enhanced cervical cancer cells viability with exposure to different concentrations of Electronic-cigarette smoke extract (E-CSE). MTT assay shows increase in cell growth at 24 hr of CSE exposure, maximum effect seen at 5% CSE (A). Alpha-Enolase expression was significantly enhanced upon treatment with various concentrations of E-CSE (B). RT-PCR analysis was conducted to confirm the data obtained from proteomic analysis. HRE Luciferase Assay revealed CSE acting similar to DMOG, an inhibitor of HIF-PH that prevents degradation of HIF-1a by prolyl-hydroxylase (C). RT-PCR analysis with HIF-1a primers demonstrated significant increase in HIF-1a mRNA expression with E-CSE treatment with varying concentrations of E-CSE (D).

An interesting fact is ENO1 gene can transcribe two proteins: a longer Enolase protein and a shorter MBP-1(c-myc binding protein) protein. By using an alternative translation start codon, ENO1 transcripts, which encode the full length polypeptide of about 48 kDa, can also be translated into a shorter protein (37 kDa), called Myc promoter-binding protein-1 (MBP-1) [37], which acts as a negative regulator of c-myc gene expression by interacting with the major promoter. In lung cancer, ENO1 and MBP-1 are regulated by discrete pathways in tumor cells. They express higher levels of ENO1 and lower levels of MBP-1. MBP-1 binds to c-myc promoter to inhibit its activity and tumour progression. What factors determine such control of one gene expressing two proteins with opposite functionality has to be determined, especially with cigarette smoke exposure? So far, several MBP-1-associated proteins have been identified, including histone deacetylase HDAC1, MIP2A/sedlin, MEK5α, NS1-BP, and the Notch1 receptor intracellular domain. The target genes of MBP-1 transcriptional activity remain unclear except for c-myc and, as recently reported, COX2. It has been reported that MBP-1 may regulate target genes at least in part through the p53–p21 pathway. Mounting evidence indicates that both α-enolase and MBP-1 might be involved in tumorigenesis of breast carcinoma, non-small cell lung cancer, hepatitis C virus–related hepatocellular carcinoma, prostate tumour, squamous cell carcinoma and neuro blastoma. It has also been shown that MBP-1 expression reduces the invasive ability of breast cancer cells both in vitro and in a mouse model, and α-enolase may participate in the control of epithelial to mesenchymal transitions [37]. While the role of the exogenous expression of MBP-1 in transcription and cell growth regulation appears to be established, the in vivo function of this protein is poorly understood.

We found different concentrations of CSE exerting different expression levels of MBP-1 and ENO1 (data not shown), warranting a thorough investigation of entire pathway. We are conducting further studies to elucidate the paths taken up by cancer cells to protect themselves and to continue with tumor progression and metastasis. When does a cancer cell bypass MBP-1 expression over enolases to support transformed state of a cancer cell will make an interesting study.

Conclusion

Cigarette smoke extract, in specific, nicotine from Reference-cigarettes and E-cigarettes induce alpha-enolase dependent glycolytic pathway by regulating the function of prolyl-hydroxylases. This in turn stabilizes HIF-1a keeping a hypoxic niche to promote tumorigenesis and metastasis in cancers. Enolases have been implicated in multiple diseases of varying organs. It can be developed as a biomarker for some cancers and become a reliable drug target in some cancers. It plays a role in muscular diseases, neuronal diseases and at the same time, maintains stemness in cells through increased glycolytic activity. However, its role in cancer stem cells needs to be elucidated. This could mean maintaining a balance between glycolysis and oxidative phosphorylation. Whether enolases determine this or not needs to be elaborately investigated. Do enolases help in converting cancer cells to cancer stem cells or does hypoxia lead to enhanced expression of enolases and a simultaneous increase in glycolytic activity in cancer stem cells in response to cigarette smoke exposure or nicotine exposure also needs to be investigated. Targeting both HIF-1 and ENO1 in combination with therapeutic intervention might give a protective advantage against tumor formation and progression due to cigarette smoking.

References

1. Noemí Rojas-Cisneros, Rony Ruíz-Saucedo (2021) Tobacco Consumption and cervical intraepithelial neoplasia. Rev. Fac. Med. Hum 21: 157-168.
2. A Rodgman (1998) Letters to the editor, Tobacco smoke components. Beitr. Tabaksforsch. Int. 18: 49–52.
3. Thielen A, Klus H, Muller L (2008) Tobacco smoke: unraveling a controversial subject. Exp. Toxicol. Pathol 60: 141–156.
4. Borgerding M, Klus H (2005) Analysis of complex mixtures—cigarette smoke. Exp. Toxicol. Pathol 57: 43–73.
5. Fowles J, Dybing E (2003) Application of toxicological risk assessment principles to the chemical constituents of cigarette smoke. Tob Control 12: 424-430.
6. Pfeifer GP, Denissenko MF, Olivier M, Tretyakova N, Stephen S, et al. (2002) Tobacco smoke carcinogens, DNA damage and p53 mutations in smoking-associated cancers. Oncogene 21: 7435-7451.
7. Simons AM, Phillips DH, Coleman DV (1993) Damage to DNA in cervical epithelium related to smoking tobacco. British Medical Journal 306: 1444-1448.
8. Hellberg D, Nilsson S, Haley NJ, Hoffman D, Wynder E (1988) Smoking and cervical intraepithelial neoplasia: nicotine and cotinine in serum and cervical mucus in smokers and nonsmokers. American Journal of Obstetrics and Gynecology 158: 910-913.
9. Melikian AA, Sun P, Prokopczyk B, et al. (1999) Identification of benzo[a]pyrene metabolites in cervical mucus and DNA adducts in cervical tissues in humans by gas chromatography-mass spectrometry. Cancer Letters. 146: 127-134.
10. Prokopczyk B, Cox JE, Hoffmann D, Waggoner SE (1997) Identification of tobacco-specific carcinogen in the cervical mucus of smokers and nonsmokers. Journal of the National Cancer Institute 89: 868-873.
11. Alam S, Conway MJ, Chen HS, Meyers C (2008) The cigarette smoke carcinogen benzo[α]pyrene enhances human papillomavirus synthesis. Journal of Virology 82: 1053-1058.
12. Gritz ER, Dresler C, Sarna L (2005) Smoking, the missing drug interaction in clinical trials: ignoring the obvious. Cancer Epidemiology Biomarkers and Prevention 14: 2287-2293.
13. Kim JW, Dang CV (2005) Multifaceted roles of glycolytic enzymes. Trends Biochem Sci 30: 142–150.

14. Liu KJ, Shi N (2007) The role of enolase in tissue invasion and metastasis of pathogens and tumor cells. J Cancer Mol 2: 45-48.

15. Pancholi V (2001) Multifunctional alpha-enolase: its role in diseases. Cell Mol Life Sci 58: 902-920.

16. Peebles KA, Duncan MW, Ruch RJ, Malkinson AM (2003) Proteomic analysis of a neoplastic mouse lung epithelial cell line whose tumorigenicity has been abrogated by transfection with the gap junction structural gene for connexin 43, Gja1. Carcinogenesis 24: 651-657.

17. Zhang L, Cilley RE, Chinoy MR (2000) Suppression subtractive hybridization to identify gene expressions in variant and classic small cell lung cancer cell lines. J Surg Res 93: 108-119.

18. Wu W, Tang X, Hu W, Lotan R, Hong WK, et al. (2002) Identification and validation of metastasis-associated proteins in head and neck cancer cell lines by two-dimensional electrophoresis and mass spectrometry. Clin Exp Metastasis 19: 319-326.

19. Hennipman A, van Oirschot BA, Smits J, Rijksen G, Staal GE (1988) Glycolytic enzyme activities in breast cancer metastases. Tumour Biol 9: 241-248.

20. Altenberg B, Greulich KO (2004) Genes of glycolysis are ubiquitously overexpressed in 24 cancer classes. Genomics 84: 1014-1020.

21. Tomaino B, Cappello P, Capello M, Fredolini C, Sperduti I, et al. (2010) Circulating autoantibodies to phosphorylated alpha-enolase are a hallmark of pancreatic cancer. J Proteome Res.

22. Bachtiary B, Schindl M, Pötter R, Dreier B, Knocke TH, et al. (2003) Overexpression of Hypoxia-inducible Factor 1α Indicates Diminished Response to Radiotherapy and Unfavorable Prognosis in Patients Receiving Radical Radiotherapy for Cervical Cancer. Clinical Cancer Research 9: 2234-2240.

23. Luppi F, Aarbiou J, van Wetering S, et al. (2005) Effects of cigarette smoke condensate on proliferation and wound closure of bronchial epithelial cells in vitro: Role of glutathione. Respir Res 6: 140.

24. Rizwani W, Aneesa F, Deepshikha S, Divya JR, Nabil AMBO, et al (2014) S137 phosphorylation of profilin 1 is an important signalling event in breast cancer progression. PloSOne 9: e103868.

25. Dasgupta P, Rizwani W, Pillai S, et al. (2009) Nicotine induces cell proliferation, invasion and epithelial-mesenchymal transition in a variety of human cell lines. Int. J. of Cancer 124: 36-45.

26. Altenberg B, Greenlich KO (2004) Genes of glycolysis are ubiquitously overexpressed in 24 cancer classes. Genomics 84: 1014-1020.

27. Fu QF, Liu Y, Fan Y, Hua SN, Qu HY, et al. (2015) Alpha-enolase promotes cell glycolysis, growth, migration and invasion in non-small cell lung cancer through FAK-mediated PI3K/AKT pathway. J. Hematol Oncol 8: 22.

28. Chang GC, Liu KJ, Hsieh CL, Hu T, Charoenfuprasert S, et al. (2006) Identification of α-Enolase as an Autoantigen in Lung Cancer: Its Overexpression Is Associated with Clinical Outcomes. Clin Cancer Res 12: 5746-5754.

29. Chu PY, Hsu NC, Liao AT, Shih NY, Hou MF, et al. (2011) Overexpression of alpha-enolase correlates with poor survival in canine mammary carcinoma. BMC Vet Res 7: 62.

30. Rizwani W (2021) Enolase: A common factor to cancer cells and stem cells, yet with divergent function in response to ROS. (Book Chapter), S.Chakraborti et al (eds) Handbook of Oxidative Stress and Cancer, Springer Publications.

31. Santana-Rivera Y, Rabelo-Fernández RJ, Quiñones-Díaz BI, Grafals-Ruíz N, Santiago-Sánchez G, et al. (2020) Reduced expression of enolase-1 correlates with high intracellular glucose levels and increased senescence in cisplatin-resistant ovarian cancer cells. Am J Transl Res 12: 1275-1292.

32. Takikita M, Altekruse S, Lynch CF, Goodman MT, Hernandez BY, et al. (2009) Associations between selected biomarkers and prognosis in a population-based pancreatic cancer tissue microarray. Cancer Res 69: 2950-2955.

33. Saggar JK, Yu M, Tan Q, Tannock IF (2013) The tumor microenvironment and strategies to improve drug distribution. Front Oncol 3: 154.

34. Jaakkola P, Mole DR, Tian YM, et al. (2001) Targeting of HIF-1 to the von Hippel Lindau ubiquitylation complex by O2-regulated prolyl hydroxylation. Science 292: 468-472.

35. Brassart-Pasco S, Brézillon S, Brassart B, Ramont L, Oudart JB, et al. (2020) Tumor Microenvironment: Extracellular Matrix Alterations Influence Tumor Progression. Front. Oncol: 10.

36. Michiels C, Tellier C, Feron O (2016) Cycling hypoxia: a key feature of the tumor microenvironment. Biochim Biophys Acta Rev Cancer 1866: 76-86.

37. Mariavera Lo Presti, Arianna Ferro, Flavia Contino, et al. (2010) Myc Promoter-Binding Protein-1 (MBP-1) Is a Novel Potential Prognostic Marker in Invasive Ductal Breast Carcinoma. PLOS ONE 5: e12961.